Direction Finding Errors Induced by Plasmawaves of the Ionosphere

Stefan Hawlitschka
FGAN-FKIE-FE
Neuenahrer Str.20
D-53343 Wachtberg-Werthhoven
GERMANY

hawi@fgan.de

ABSTRACT

A super-resolution high frequency (HF) direction finding (DF) system has been used to measure the temporal characteristics of mid-latitude ionospheric irregularities. By analysis of the log power spectrum of the temporal profiles they are classified into six classes: (1) traveling wave packets (TWPs), (2) wave trains (WTs), (3) large-scale traveling disturbances at the terminator (TLSTIDs), (4) interference of different waves (IDW), (5) chaos and (6) quiet state. Their occurrence is correlated to the time of day, the ionospheric layer of reflection and the geomagnetic conditions which are expressed by the local K index. In total 192.25 hours of observation have been processed with a newly developed super-resolution DF algorithm which is suited for direction finding of moving incidence angles.

1.0 INTRODUCTION

One of the main concepts in recent ionospheric research is to describe ionospheric irregularities as plasmawaves [1-5]. A classification according to their periods and generating mechanisms is common even though varying slightly in the literature: Planetary waves (PWs) with periods from 24 hours on, sunset and dawn effect with a period of 24 h and its harmonics, large-scale traveling ionospheric disturbances (LSTIDs) with periods from 30-60 min up to several hours and medium-scale traveling ionospheric disturbances (MSTIDs) with periods from about 6-10 min up to 40-60 min. Small-scale traveling ionospheric disturbances (SSTIDs) and other irregularities on the shortest scale are not investigated in this study, on the contrary the applied DF algorithm is designed to filter them out. It is generally accepted that LSTIDs are generated by specific geophysical events like ionospheric substorms of the auroral oval of the northern and southern hemisphere [2,7,8]. Local pressure gradients are generated due to Joule heating and particle precipitation. These gradients at the auroral zone cause an equator-ward neutral wind that interacts with the plasma [9]. The source mechanisms of MSTIDs, however, are not consistently described. Some authors contribute their origin to the auroral zone [3,7] while others describe them as manifestations of meteorological processes and their occurrence as far more frequent than the occurrence of geomagnetic storms [1,9]. Afraimovich even enumerates many possible sources of MSTIDS: magnetic storms, auroral phenomena, weather factors, tropospheric turbulence and jet flows, the solar terminator, strong earthquakes, volcanic eruptions and anthropogenic influences as rocket launches, explosions and nuclear tests [10]. He even found a possible anti missile strike in the atmosphere as a source of TIDs and estimates the location of the explosion [11]. Due to these many generation mechanisms single MSTIDs have rarely been identified but mostly a mixture of multiple MSTIDs has been identified. Traveling wave packets consisting in several quasi-monochromatic periods of a MSTID have been described as rare events, in a study by Afraimovich et al. they could be identified in only 0.1-0.4 % of all observations [4,10]. LSTIDs have commonly been observed as “wave trains” with several

Hawlitschka, S. (2006) Direction Finding Errors Induced by Plasmawaves of the Ionosphere. In *Characterising the Ionosphere* (pp. 16-1 – 16-14). Meeting Proceedings RTO-MP-IST-056, Paper 16. Neuilly-sur-Seine, France: RTO. Available from: http://www.rto.nato.int/abstracts.asp.

periods. The purpose of this paper is to investigate the occurrence of well pronounced waves compared to the “mixed” state “chaos” when many different waves interfere and no individual wave can be identified what is also the case for a quiet ionosphere. As a “medium” state the class of interfering of different waves (IDW) is introduced where the number of interfering waves is sufficiently small so that the individual interfering waves can be identified.

A high frequency (HF) narrowband direction finding (DF) system has been used to record data in three measurement campaigns. Narrowband means that the bandwidth is adapted to receive one source. Nonetheless the HF band is dense populated so that cochannel interferences usually are encountered. Additionally two way propagation can occur because of the reflection of the HF signal of one source on two ionospheric layers. By the use of super-resolution DF algorithms the multiple waves incident onto the antenna array could be resolved in the far most recordings. For this study the incidence angles of mostly radio stations are estimated [6]. During their passage through the ionosphere the HF-waves are deviated by the free electrons of the plasma of the ionosphere. When the density of free electrons is high enough the HF waves are “reflected” what is the basic principle for worldwide HF communication. But the ionosphere normally is not a perfect plane mirror. Moving ionospheric irregularities of the electron content pass the “reflection point” and cause deviations of the propagation path of the HF waves from great circle propagation. These deviations are observed and their characteristics are evaluated by analysis of the temporal power spectra in the period range from several minutes to several hours. Large-scale traveling ionospheric disturbances (LSTIDs) have been found in a previous study by analysis of the log power spectrum of the time series of the bearing angle and their appearance was in most cases connected with geomagnetic activity [5]. For MSTIDs the picture was not clear. They appeared in every observation with a continous spectrum. Their occurrence may have been masked by the big spread of bearing angles. With the application of recently developed super-resolution algorithms for moving incidence angles their spread could be considerably reduced. The combined estimation of several covariance matrices of the received data [6] together with a kalman filter [12] “focuses” the temporal profiles to the traces of the TIDs. Thus a new analysis of the occurrence and the characteristics of ionospheric irregularities has been conducted observing sources with known locations such as radio stations in mid-latitudes [6]. But on the contrary to the previous study [5] identifiable TIDs are now discriminated according to a new systemtics: *traveling wave packets* (TWPs) [4,10], *wave trains* (WTs), *terminator large-scale TIDs* (TLSTIDs) [14,15], *interferences of different waves* (IDWs), *chaotic* behaviour or if the ionosphere is comparably *quiet*. TWPs are a monochromatic or quasi-monochromatic TID with several periods, WTs equally exhibit several periods of different frequency and an IDW event is composed of several interfering waves which are nonetheless well pronounced in the spectrum and well visible in the temporal profile of the bearing. The shortest time-scale that has been investigated is 10 minutes whereas the longest large-scale TID (LSTID) was three hours. For this study the time series and their power spectra of recordings with a total duration of 192.25 hours have been analyzed. The elevation angles were used to determine whether E-region or F-region reflection occurred. To detect favorable conditions for their existence the appearance of the phenomena has been tabled against the local K index, the reflection layer and the time of day. The time of day has been divided into six classes: Morning, forenoon, noon, afternoon, evening and night. As the purpose is to investigate ionospheric processes dependent on the ionospheric state, the *ionospheric morning* and *evening* have been defined as the time when the F-layer descends or raises respectively. This is essentially the transition time between the daytime and the nighttime ionosphere and vice versa. The effect is that for example in November on the northern hemisphere the *ionospheric evening* usually begins earlier when direction finding a station in north-east direction than in south-west direction. Depending on the dissipation rate of ionization in the F-region the beginning and the end of the *ionospheric evenening* may vary from day to day. Afternoon and night are just before or after evening. Forenoon begins when the descending of the F-Layer has been completed. As noon has been denoted the time from 12-14 h local time (LT).

2.0 INSTRUMENTATION

A super-resolution DF system has been operated as a single station locator. The system has ten active antennas which are grouped on two concentric circles with five antennas respectively. This assures omnidirectional sensitivity of the antenna array. The inner circle has a radius of 30.5 m the outer radius is 65 m. The antenna signals are fed into a 10-channel receiver, mixed to an IF and digitized. Then they are digitally downconverted and fed into an desktop computer where their covariance matrices are calculated. These are stored on the hard drive for offline processing in the office. The directions of reception are calculated on a desktop computer with a super-resolution DF algorithm for moving sources [6] which has been combined with a Kalman filter approach [12]. The temporal evolution of the bearing angles is evaluated by (1) analyzing the variation of the bearing compared to the “true” direction and (2) analyzing the temporal spectrum of the bearing variations. The layer of reflection has been estimated using the elevation angles and simple geometric considerations. In some cases the results have been checked with the radio circuit calculation program ICEPAC [13].

3.0 DATA

Three measurement campaigns have been carried out from 6-9 November 2001, 15-25 April 2002 and 14-15 May 2002 (all the data and their analysis is listed in table 5 in the appendix). The intraday distribution of the K indices and layers of reflection are shown in the appendix in tables 6 and 7. The aim is classify plasmawaves according to the systematics as described in Section 1.0 and to study their frequency of occurrence. The recording from the evening of 23.4.02 to the forenoon of 24.4.02 has been selected for a showcase analysis like it has been carried out for all the observations (see table 5 for details). The temporal profile of the bearing can be seen in figure 1. The DF system had been located at Greding near Nuremberg in Germany. The emitter is a weather service from DWD at Pinneberg near Hamburg / Germany, the frequency of the emitter is 7.646 MHz. Due to the relatively high frequency there is no reception at night. The data set has been divided into three parts: the evening / night part (figures 2 and 3) from the beginning of the recording until 23 h, the passage of the terminator LSTID (figures 4 and 5) in the morning from 6.5 h to 7.3 h and the forenoon (figures 6 and 7) from 7.5 to 10 h. For every pair of figures on the left side the temporal profile and on the right side the log power spectrum is arranged. For analysis of the periods of the plasamwaves first the temporal profile is inspected visually. Then the power spectrum is calculated for intervals where constant behaviour is found.

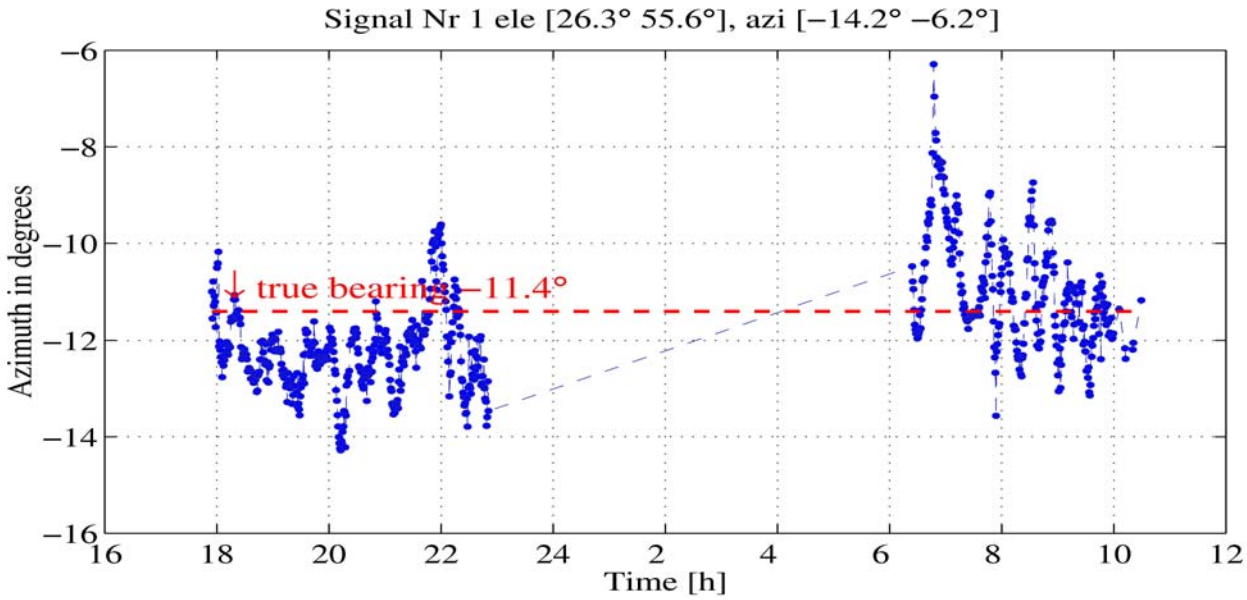

Figure 1: Bearing of the emitter of DWD in Pinneberg / northern Germany, the DF system was located in Greding near Nuremberg. The frequency is 7.646 MHz. Due to the relatively high frequency there is no reflection of the HF waves from 23 to 6 h local time. From 18 h to 23 h wave trains have appeared, in the morning a terminator LSTID appears followed by a TWP.

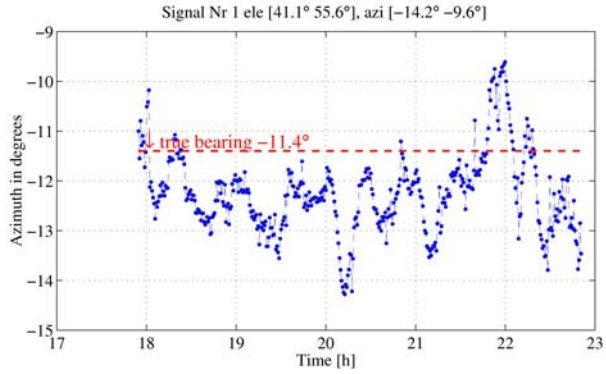

Figure 2: Temporal profile of the bearing from 17.9 h to 23 h. Well pronounced plasmawaves are recognizable.

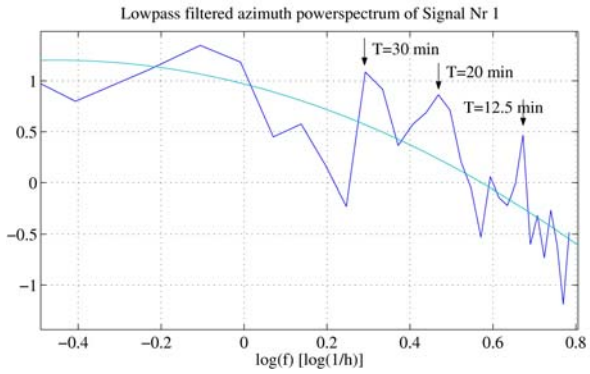

Figure 3: Associated log power spectrum to the temporal profile of figure 2. A polynomial of second degree has been fitted to the data. Peaks exceeding the line indicate the most prominent waves in figure2.

In figure 2 the evening / night part of the data set is shown. Well pronounced plasmawaves are visible and are analyzed in the associated log power spectrum in figure 3. A polynomial of second degree has been fitted to the power spectrum. It is assumed from a previous study [5] that this is the typical shape of the spectrum as long as no large-scale TIDs pass the reflection point of the HF-waves. It is taken as a continous background spectrum. Therefore the peaks exceeding the fitted line specify individual ionospheric waves. There are three different peaks in the spectrum. Due to the logarithmic scaling of the spectrum the period T of a specific wave can be calculated as

$$T[\mathrm{min}] = 60/10^{\log(f)}.$$

The dominant periods in figure 3 are readily calculated as 30 minutes, 20 minutes and 12.5 minutes. They can be identified in figure 2 with individual waves which follow each other in a casual way, but do not interfere much. Thus the temporal profile is classified as a *wave train*. The long term deviation with 4 hour period is no TID but a "*sunset-effect"* which appears when the F layer moves up to nighttime heights [5]. In the connecting area between daytime and nighttime ionosphere the F layer is tilted. The effect starts at 18 h and ends at 22 h. The wave train persists the whole timed interval.

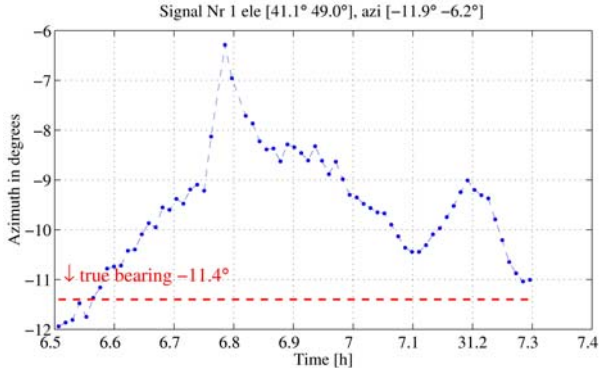

Figure 4: Signature of the passage of a LSTID on the morning of 24.4.02. From 7.1 to 7.3 h additionally a MSTID passes.

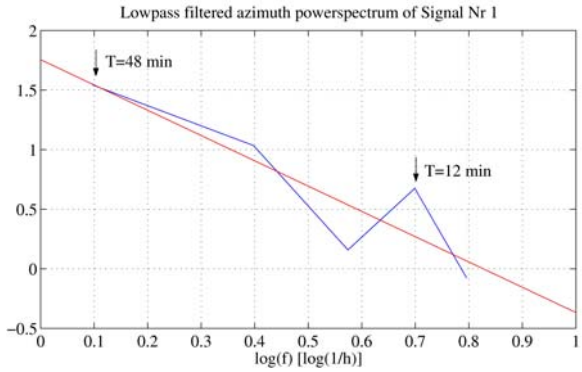

Figure 5: Associated log power spectrum to the temporal profile of figure 4.

In figure 4 the passage of a LSTID at the terminator can be identified. Some authors state that the terminator is the most probable generating source and describe them as *terminator driven* [14,15]. The background spectrum when LSTIDs are present has been assumed to be approximated by a straight line [5]. The period has been determined to be about 48 min, nonetheless the power spectrum at this point doesn't exceed the fitted line because there are too few data points and the period lies at the end of the spectrum. From 7.1 to 7.3 h passes an additional MSTID with 12 minutes period. The "hat" at 6.8 h could not be interpreted.

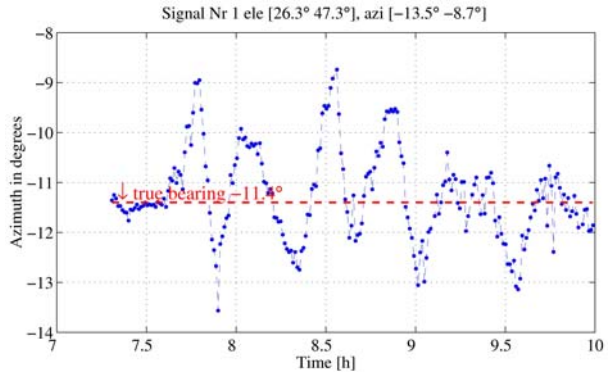

Figure 6: Signature of a traveling wave packet on the forenoon of 24.4.02

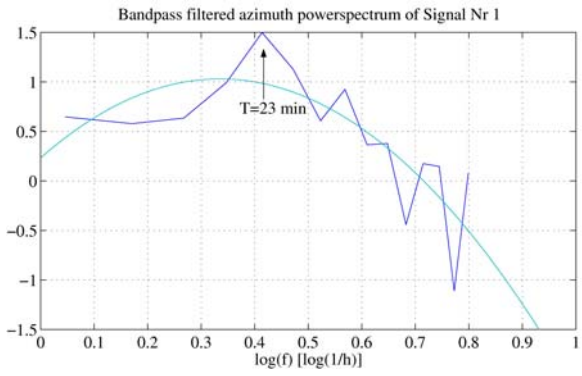

Figure 7: Associated log power spectrum to the temporal profile of figure 6.

In figure 6 the passage of a quasi-monochromatic *traveling wave packet* is shown. In the spectrum a broad peak can be identified indicating that the frequency may not be "sharp" or that it doesn't lie on the raster of the FFT. Since different rasters have been tried, it is most probable that the period of the plasmawave changes slightly from cycle to cycle and after 9 h it seems to augment.

The three classes not disccussed in the example are classified as follows: *Interference of different waves* (IDW) has several interfering waves, in contrary to the wave train where distinct waves follow each other. The spectrum maybe similar in both cases, the difference is however that in the IDW they interfere. But it differentiates from the classes *chaos* and *quiet* in that there are pronounced, identifiable waves. *Chaos* and *quiet* state show a nearly continuous spectrum with all periods contained and the shape of the spectrum is appromimately that of the background spectrum. The difference between *chaos* and *quiet* is determined by the energy in the spectrum leading to higher values for the class *chaos*. Accordingly the spread of bearings is considerably higher than at quiet ionosphere where the spread may be less than half a degree.

4.0 RESULTS

A total of 192.25 hours of observations has been investigated. In this section the results of the statistical analysis of the occurrence of the different classes of the classification scheme from Section1 are shown.

In table 1 the number of occurrences of ionospheric irregularities are displayed. Their occurrence is investigated including the intraday variation of their occurrence. The course of a day is divided into the six classes *morning*, *forenoon*, *noon*, *afternoon*, *evening* and *night*. Additionally the dependence of the appearing of irregularities on the layer of reflection (E or F layer) and on the geomagnetic index (*K=1…3*, *K=4—5*, *K>5*) is analyzed. The data has been arranged based on the data in table 5 in the appendix. A total of 73 observations has been extracted from the 192.25 hours of recording such that each ionospheric event has been counted once each time of day it occurred. For instance when a wave train has persisted from the evening into the night, it has been counted as one wave train on the evening and one wave train at night. More illustrative however is the representation of the data in percent values (table 2). The total number of events in a column is again given in row 2. It should be noted that the sample size of some classes is relatively small. Even though one event may represent several hours of data, there exists a considerable uncertainty if a generalization of the results is tried. But trends may be deducted in many cases. The morning observations revealed mostly *terminator driven LSTIDs* and *wave trains*. On forenoon only *quiet ionosphere* or *WTs* and *TWPs* were detected. On noon mostly *quiet ionosphere* was existent and once a *wave train* was detected. It must be stated however, that the sample size consisted only in 6 data takes. The ionosphere of the afternoon was in most observations governed by a *quiet ionosphere* or by *traveling wave packets*. In the evenings and at night *TWPs* and *WTs* were dominant. It is not surprising that the morning, evening and night observations show less *quiet* states of the ionosphere than the daytime recordings. In the next columns the distribution of events in the ionospheric layers is shown. The E-layer was in more than 50 % of all observations *quiet* whereas the F layer was dominated by *wave trains*, *traveling wave packets* and the *terminator LSTIDs*. Under quiet geomagnetic conditions (K=1—3, both layers) *wave trains* and a *quiet ionosphere* prevailed. For K=4—5 (both layers) still *quiet* conditions were present with high probability but *traveling wave packets* became more probable. With K>5 (both layers) the highly energetic events such as *TWP*, *WT*, *chaos* and *interference of different waves* prevailed.

Table 1: The number of occurrences of ionospheric irregularities from all 73 observations classified by time of day, layer of reflection and local geomagnetic index. In the first row the total number of observations of the phenomena are given.

Class	Morning	Forenoon	Noon	Afternoon	Evening	Night	E	F	K=1-3	K=4-5	K>5
Total #	9	11	6	12	17	18	17	20	33	9	6
TWP #	1	2	0	1	4	3	2	3	3	2	2
WT #	3	3	1	4	7	11	2	12	12	2	2
TLSTID #	4	0	0	0	0	0	0	3	3	1	0
Interference #	0	0	0	0	3	2	1	1	3	0	1
Chaos #	0	0	0	2	2	1	1	1	3	0	1
Quiet #	1	6	5	5	1	1	11	0	9	4	0

Table 2: Percentage values of the occurrence of the irregularities classified by time of day, layer of reflection and local geomagnetic index. For instance there have been in 61.1 % of 17 night-time observations traveling wave packets.

Class	Morning	Forenoon	Noon	Afternoon	Evening	Night	E	F	K=1-3	K=4-5	K>5
Total #	9	11	6	12	17	18	17	20	33	9	6
TWP %	11.1	18.2	0	8.3	23.5	16.7	11.8	15	9.1	22.2	33.3
WT %	33.3	27.3	16.7	33.3	41.2	61.1	11.8	60	36.4	22.2	33.3
TLSTID %	44.4	0	0	0	0	0	0	15	9.1	11.1	0
Interference %	0	0	0	0	17.6	11.1	5.9	5	9.1	0	16.7
Chaos %	0	0	0	16.7	11.8	5.6	5.9	5	9.1	0	16.7
Quiet %	11.1	54.5	83.3	41.7	5.9	5.6	64.7	0	27.3	44.4	0

Next the general and the intraday variation of the frequency of the irregularities are analyzed in table 3. The distribution of the events is given in columns two and three from a total number of observations of 73. In 15 % of all measurements *TWP*s were observed, in 40 % *wave trains*, in 5.4 % *TLSTIDs*, *interferences* and *chaos* in 6.8 % respectively and a *quiet* ionospheric state was detected in 26 % of all observations (Column 3). That means that in 67.2 % of all observations well pronounced irregularities have been found. The other columns show the intraday variation. Because the measurements were not equally distributed over the course of the day, the relative frequency based data of table 2 where taken. In the percentage values an equal sample size of 100 for each time of day is “simulated” and the data are thus normalized and comparable. The table has now to be read row-wise. The intraday distribution of the *TWP* events occurred (with the normalization as described) not at noon but preferably on the evening, the forenoon and during the night. *Wave trains* were more distributed over the day but also occurred less frequently at noon. *Terminator LSTIDs* were only found at the morning terminator but not on the evening. Interferences of different waves were only present on the evening and the night whereas *chaotic* behavior often already began in the afternoon and was less frequent in the night. *Quiet* ionosphere was a frequent state in the E layer on forenoon, noon and afternoon.

Table 3: Percentages of the occurrence of irregularities by time of day. Basis are the data of table 2 where all time of day are equally weighted what is not the case in table1. For instance a quiet ionosphere occurred preferably during morning, noon and afternoon. TLSTIDs appeared only in the morning.

Time of day	Total # (73)	Total %	Morning %	Forenoon %	Noon %	Afternoon %	Evening %	Night %
TWP	11	15	14.3	23.4	0	10.7	30.2	21.5
WT	29	40	15.6	12.8	7.8	15.6	19.4	28.8
TLSTID	4	5.4	100	0	0	0	0	0
Interference	5	6.8	0	0	0	0	61.3	38.7
Chaos	5	6.8	0	0	0	49	34.6	16
Quiet	19	26	5.5	27	41.2	20.6	2.9	2.8

Table 4: Percentages of the occurrence of irregularities by layer of reflection and by local geomagnetic index. Wave trains appeared mostly in the F layer at every geomagnetic condition whereas TWPs appeared in both layers with no clear preference and preferably at disturbed geomagnetic conditions.

Class	Total layer #	E %	F %	Total K #	K=1-3 %	K=4-5 %	K>5 %
TWP	5	44	56	7	14	34.4	51.6
WT	14	16.4	83.6	16	39.6	24.2	36.2
TLSTID	3	0	100	4	45	55	0
Interference	2	54	46	4	35.3	0	64.7
Chaos	2	54	46	4	35.3	0	64.7
Quiet	11	100	0	13	38.1	61.9	0

5.0 CONCLUSIONS

A classification of the irregularities present in the ionosphere as measured by a super-resolution DF system has been developed. Even though the sample size was quite small, our measurements revealed that we have the systematics at hand to classify most of the wave-like phenomena of the mid-latitude ionosphere. Traveling wave packets were found in 15 % of all observations which is much more frequently than in a previous study of Afraimovich [10]. He observed TWPs in only 0.1—0.4 % of all observations he conducted using GPS network data. The results presented in this paper state that the ionosphere in mid-latitude is much less chaotic and mostly contains individual waves.

6.0 OUTLOOK

Many more measurements will be undertaken in the near future to enhance the statistical significance of the observations. Additionally the spatial characteristics is of high interest. As the DF system used in this study is narrowband, only the temporal behavior of plasmawaves passing through the reflection point of the HF waves could be investigated. With our coming broadband system BRAHMS [6] even spatial investigations will be possible by combining the observations from different sources with different locations. There exist hundreds of short-wave radio stations in middle Europe with known locations. The well identifiable events as TWPs, wave trains, interferences of several waves and terminator driven LSTID will be investigated with respect to their spatial dynamic characteristics as there are the direction of the motion, propagation velocity correlation length and the source region.

7.0 REFERENCES

[1] Afraimovich, E. L., Kosogorov, E. A., Lesyuta, O. S., Ushakov, I. I., Yakovets, A. F. (2001): *Geomagnetic Control of the spectrum of travelling ionospheric disturbances based on data from a global GPS Network.* Ann. Geophys. 19, 723—731.

[2] Hocke, K., Schlegel, K. (1996): *A review of atmospheric gravity waves and travelling ionospheric disturbances: 1982—1995*. Ann. Geophys. 14, 917—940.

[3] Kalikhman, A. D., (1980): Medium-scale travelling ionospheric disturbances and thermospheric winds in the F-region. JASTP 42, 697—703.

[4] Yakovets, A. F., Kaliev, M. Z., Vodiannikov, V. V., (1999): *An experimental study of wave packets in travelling ionospheric disturbances*. JASTP 61, 629—639.

[5] Hawlitschka, S. (2006): *Travelling ionospheric disturbances (TIDs) and tides observed by a super-resolution HF direction finding system*. JASTP 68, 568—577.

[6] Baum, D., Foerster, W., Hawlitschka, S. (2006): *BRAHMS Broadband Automatic HF-Monitoring System*. NATO RTO IST-056 / RSM-002.

[7] Hunsucker, r. D. (1982): *Atmospheric gravity waves generated in the high-latitude ionosphere: A review*. Rev. Geophys. 20, 293—315.

[8] Francis, S. H. (1975) : *Global propagation of atmospheric gravity waves : A review*. JASTP 37, 1011—1054.

[9] Waldock, J. A., Jones, T. B. (1987): *Source regions of medium-scale travelling disturbances observed at mid-latitudes*. JASTP 61, 629—639.

[10] Afraimovich, E. L., Perevalova, N. P., Voyeikov, S. V. (2002): *Traveling wave packets of total electron content as deduced from global GPS network data*. JASTP 65(11-13): 1245-1262.

[11] Afraimovich, E. L., Voeykov, S. V., Lesyuta, O. S., Perevalova, N. P.,Nagorsky, P. M. (2003): *The traveling ionospheric disturbance conceivably initiated by a high altitude explosion during the testing of the US anti-missile system on July 15, 2001*. Solar terrestrial Physics, 3, Institue of Solar-Terrestrial Physics SBRAS, Irkutsk, 73—79.

[12] Hawlitschka. S. (2006): *ML super-resolution DF methods for moving sources*, To appear.

[13] Stewart, F. G.: ***I**onospheric **C**ommunications **E**nhanced **P**rofile **A**nalysis & **C**ircuit (**ICEPAC**)*, www.its.bldrdoc.gov/elbert/hf_prop/manuals/icepac_tech_manual.pdf.

[14] Boska, J., Sauli, P., Altadill, D., German Sole, J., Alberca, L. F.: *Diurnal variation of gravity wave activity at midlatitudes in the ionospheric region.* Stud. Geophys. Geodaet., 47, 579—586.

[15] Galushko, V. G., Paznukhov, V. V., Yampolski, Y. M, Foster, J. C. (1998): *Incoherent scatter radar observations of AGW/TID events generated by the moving solar terminator*. Ann. Geophys. 16, 821—827.

APPENDIX

Table 5 displays all used observations and the ionospheric characteristics deduced from them. In the first column the date of the recording is given. Then the station which has been received is specified if known or it is specified as a cochannel interferer. The next column indicates the HF-frequency of the emission. Then the true bearing, or in the case of a cochannel interferer the estimated “true” bearing is given. Column 5 contains the beginning and the end time of the observation. For easier comprehension the numbers are highlighted with colors as follows: Morning – red, Forenoon – light red, noon – light yellow, afternoon – dark yellow, evening – light blue, night – dark blue. All times are local times. Then the duration of the recording is indicated. The observations are part of longer recordings and have been divided according to the observed phenomena so that each observation is a uniform event. The dominant ionospheric irregularities -as given in Section 1.0- are specified in columns 7-12 and depending on the phenomenon the period is specified or where applicable the occurrence is marked with an bold **X**. The layer of reflection is indicated in column 13. Additionally the rows have been colored accordingly with light red for F-Layer reflection and light yellow when E-layer reflection occurred. Then the local K index as provided from GFZ Potsdam is given. Last some remarks are given. This table is the basis for the analysis given in tables 1—4.

Below the total observation time of the ionospheric phenomena is given. First for all observations together, then for F-layer and E-layer reflection separately.

Table 5: Analysis of the measurements. Description is given in the text.

Date	Station	Freq [MHz]	Dir [°]	Time [LT]	Length [h]	TWP [min]	Wave Train [min]	Terminator LSTID [min]	Interference	Chaos	Quiet	Layer	Local K index	Remarks
6.11.01	DLF Berlin	6.005	19.3	17.5-21.5	4	**45**						F	6	
7.11.01	Cochannel Interf.	6.005	0 est	2-5	3	**25-31**						?	5	
7.11.01	Cochannel Interf.	6.005	0 est	5-7	2						**X**	?	3	
7.-8.11.01	Meteo Roma	5.8875	173.1	17.3-2.5	9	**150+75**						E-F	2-3	Weak TWP
8.11.01	Meteo Roma	5.8875	173.1	5-8.5	3.5			**90+120**				F-E	2-1	
8.11.01	RF Pori	6.120	21	17-24	7		**75+48+22**					F	0-2	
9.11.01	Coch. Int.	6.120	114 e	0-6	6					**X**		?	1	
15.4.02	RN Flevo	5.955	313.7	15-19	4					**X**		E	2	E-layer disintegrating
16.4.02	RN Flevo	5.955	313.7	7-8	1			**90-120**				F	2	Beginning not received
16.4.02	RN Flevo	5.955	313.7	8-16	8						**X**	E	1-2	8-11 formation of E
16.-17.4.02	DLF Berlin	6.005	19.3	16.3-5	12.7		**LS- + MSTIDs**					F	2-3	LSTID stronger at night
17.4.02	DLF Berlin	6.005	19.3	8-11	3		**60+24**					F	2	
17.4.02	DW Wertachtal	6.075	204.6	15.5-20	4.5		**Sporadic MSTIDs**			**X**		F	5-7	
17.-18.4.02	Cochannel Interf.	6.075	240 e	22-8	10		**LSTIDs**					?	3-6	
18.4.02	DW Wertachtal	6.075	204.6	8.5-10.5	4						**X**	E	4	
18.4.02	DW Wertachtal	6.075	204.6	12-15	3		**40+25+15**					F	3-4	
18.4.02	DWD Pinneberg	4.583	348.6	14.7-18.5	3.7						**X**	E	3	
18.4.02	DWD Pinneberg	4.583	348.6	18.5-21	2.5					**X**		E-F	3	Transition from E to F
18.-19.4.02	DWD Pinneberg	4.583	348.6	21-6	9		**50+40**					F	3-5	
19.4.02	DWD Pinneberg	4.583	348.6	6-8	2						**X**	E	3	Transition from F to E
19.4.02	Meteo Roma	5.8875	173.1	12.3-13.5	1.2						**X**	E	5	
19.4.02	Meteo Roma	5.8875	173.1	17.3-19.5	2.2						**X**	E	5	Transition from E to F
19.4.02	Meteo Roma	5.8875	173.1	19.5-24	4.5				**134+34+25**			F	5-6	
20.4.02	Meteo Roma	5.8875	173.1	6-13	7						**X**	E	5	
20.4.02	Meteo Roma	5.8875	173.1	15-21	6	**36**						E	4-6	Weak TWP

Date	Station	Freq [MHz]	Dir [°]	Time [LT]	Length [h]	TWP [min]	Wave Train [min]	Terminator LSTID [min]	Interference	Chaos	Quiet	Layer	Local K index	Remarks
20.4.02	Meteo Roma	5.8875	173.1	21-24	3				**36+60**			F	5-3	
21.4.02	Meteo Roma	5.8875	173.1	6-10	4		**Sporadic 34+20**					E	1	
21.4.02	Meteo Roma	5.8875	173.1	12.5-15.5	3						**X**	E	1	
21.4.02	Meteo Roma	5.8875	173.1	18-24	6		**6 periods**					F	1-3	
22.4.02	Meteo Roma	5.8875	173.1	4.5-7.5	3			**100**				F	3	
22.4.02	Meteo Roma	5.8875	173.1	8.1-10.5	1.6						**X**	E	2	
22.4.02	Cochannel Interf	5.8875	324 e	11-13.5	2.5						**X**	F(?)	2	
22.4.02	Meteo Roma	5.8875	173.1	14.8-16	2.2						**X**	E	3	
22.4.02	DWD Pinneberg	4.583	348.6	17.75-20	2.25		**34+11**					E	3	
22.4.02	DWD Pinneberg	4.583	348.6	20-24	4		**20…85**					F	2	Mostly non interfering
23.4.02	DWD Pinneberg	4.583	348.6	0-5	5		**80+40**					F	1-2	
23.4.02	DWD Pinneberg	4.583	348.6	5-6.5	1.5			**90**				F	4	
23.4.02	DWD Pinneberg	4.583	348.6	7-9.5	2.5	**20**						E	4-5	Weak TWP
23.4.02	DWD Pinneberg	7.646	348.6	18-23	5		**30+20+13**					F	4-2	
24.4.02	DWD Pinneberg	7.646	348.6	6.5-7.5	1			**50+MS 12**				F	2	MSTID interfering
24.4.02	DWD Pinneberg	7.646	348.6	7.5-10	2.5	**23**						F	1	6 periods
24.4.02	DWD Pinneberg	10.100	348.6	17.3-22.3	5		**60…12**					F	2-1	Mostly non interfering
25.4.02	Cochannel Interf	10.100	240 e	3-10	7		**90+30+20+12**					?	1-0	Mostly non interfering
14.5.02	DLF Berlin	6.005	19.3	19-20.1	1.1	**16**						F	3	4 periods
14.5.02	DLF Berlin	6.005	19.3	20.1-21.2	1.1				**33+13**			F	5	
14.5.02	DLF Berlin	6.005	19.3	21.4-22.9	1.5				**90+30**			F	5	weak MSTID
14.-15.5.02	DLF Berlin	6.005	19.3	22.9-2	3.1		**60+30+26**					F	4	
15.5.02	DLF Berlin	6.005	19.3	8.4-10	1.6						**X**	E	2	
Total [h]				**0-24**	**192.25**	**28.1**	**88.3**	**10**	**10.1**	**14.75**	**41**	**E+F**	0-7	

Direction Finding Errors Induced by Plasmawaves of the Ionosphere

Date	Station	Freq [MHz]	Dir [°]	Time [LT]	Length [h]	TWP [min]	Wave Train [min]	Terminator LSTID [min]	Interference	Chaos	Quiet	Layer	Local K index	Remarks
Total [%]				**0-24**	**100**	**14.6**	**46**	**5.2**	**5.2**	**7.7**	**21.3**	**E+F**	0-7	
Total [h]				**0-24**	**91.5**	**7.6**	**65.05**	**6.5**	**10.1**	**2.25**	**0**	**F**	0-7	
Total [h]				**6-21**	**55.2**	**8.5**	**6.25**	**0**	**0**	**4**	**36.5**	**E**	1-6	
Total [%]				**0-24**	**100**	**8.3**	**71.1**	**7.1**	**11**	**2.5**	**0**	**F**	0-7	
Total [%]				**6-21**	**100**	**15.4**	**11.3**	**0**	**0**	**7.2**	**66.1**	**E**	1-6	

Table 6: Intraday distribution of the measurement conditions. The total number of E and F layer observations is smaller compared to the sum of total observations because not in alls cases a reflection layer could be certainly determined.

Time of day	Total #	Morning %	Forenoon %	Noon %	Afternoon %	Evening %	Night %
K=1..3	44	7	7	2	8	8	12
K=4—5	19	3	3	3	2	3	5
K>5	10	1	0	0	2	4	3
E layer	25	3	7	4	8	3	0
F layer	44	4	2	1	3	11	23

Table 7: Intraday distribution of the measurement conditions. The total number of E and F layer observations is smaller compared to the sum of total observations because not in all cases a reflection layer could be certainly determined. Percentages are calculated from table 7 in the appendix. High K indices are not found on forenoon and noon. E layer reflection occurred preferably on daytime and not at night. Most of the F layer reflection observations were taken on the evening and night time.

Time of day	Total #	Total %	Morning %	Forenoon %	Noon %	Afternoon %	Evening %	Night %
All K	73	100	12.3	15.1	8.2	16.5	23.2	24.7
K=1..3	44	60.3	15.9	15.9	4.5	18.2	18.2	27.3
K=4—5	19	26	15.8	15.8	15.8	10.5	15.8	26.3
K>5	10	13.7	10	0	0	20	40	30
E layer	25	36.2	12	28	16	32	12	0
F layer	44	63.8	9.1	4.5	2.3	6.8	35	52.3